Title

Xenopus CENP-A assembly into chromatin requires base excision repair proteins

Author

Zeitlin, Samantha G

Publication Date

2005-02-25

DOI

10.1016/j.dnarep.2005.02.007

Peer reviewed

3/11/05

Xenopus CENP-A assembly into chromatin requires base excision repair proteins

Samantha G. Zeitlin*[1], Sheetal Patel[1], Bodil Kavli[2] and Geir Slupphaug[2]

1. Department of Biological Sciences, University of California San Diego, La Jolla, CA 92093

2. Faculty of Medicine, Institute for Cancer Research & Molecular Medicine, NTNU, N-7489 Trondheim, Norway

***Corresponding author:**

szeitlin@biomail.ucsd.edu, tel: (858) 534-2828

Abstract

CENP-A is an essential histone H3 variant found in all eukaryotes examined to date. To begin to determine how CENP-A is assembled into chromatin, we developed a binding assay using sperm chromatin in cell-free extract derived from Xenopus eggs. Our data suggest that the catalytic activities of an unidentified deoxycytidine deaminase and UNG2, a uracil DNA glycosylase, are involved in CENP-A assembly. In support of this model, inhibiting deoxycytidine deaminase with zebularine, or uracil DNA glycosylase with Ugi, uracil or UTP results in a lack of detectable CENP-A on sperm DNA. Conversely, inducing DNA damage increases the level of CENP-A detected on sperm chromatin. Our data suggest that base excision repair may be involved in assembly of this histone H3 variant.

1. Introduction

CENP-A is an essential histone H3 variant found in all eukaryotes examined to date[1-4]. Bulk chromatin, containing the four core histones, H3, H4, H2A and H2B is assembled during S phase, just behind the replication fork (reviewed in [5,6]). In contrast, it has been shown that CENP-A assembly is uncoupled from DNA replication. Although the peak of endogenous CENP-A assembly probably occurs during G2, epitope-tagged CENP-A can be assembled throughout the chromatin, and at any time during the cell cycle [7].

In Xenopus eggs, maternal histones are stored in large quantities in the cytoplasm [8]. The Xenopus egg extract system is competent for DNA replication, repair, and chromatin assembly. When purified sperm nuclei are combined with egg cytoplasm and nuclear membranes, the sperm go through a dramatic decondensation process, assemble chromatin, and form nuclei. In this system, DNA replication is very rapid, allowing for efficient analysis of interphase events [9].We chose Xenopus egg extract as a model system in which to investigate how CENP-A is assembled onto sperm chromatin.

During spermatogenesis, most sperm histones are replaced with small, basic proteins called protamines. Despite the replacement of most paternal histones with protamines, CENP-A is selectively retained in sperm [10]. To begin to study how CENP-A is localized on DNA in the nucleus, we developed a binding assay using Xenopus sperm and cell-free S-phase extract derived from Xenopus eggs. In the course of these studies, we observed that CENP-A assembly is apparently very dynamic, and can be modulated by the presence or absence of active DNA repair machinery.

2. Materials and Methods

2.1 DNA sequences

DNA sequencing was performed by the DNA Sequencing Shared Resource, UCSD Cancer Center. The XCENP-A cDNAs were obtained from the I.M.A.G.E bank at Research Genetics (Genbank accession numbers BG408673 and BE679671). For initial confirmation, sequences were aligned with CLUSTALW as part of the Biology workbench package at the UCSD Supercomputer Center. Alignment shown in Figure 1 was generated and edited manually using XCED [11].

2.2 Preparation of Xenopus egg extracts and sperm nuclei

Xenopus high-speed interphase extracts were generated using an updated version of a method described previously [9]. Adult Xenopus females were primed with pregnant mare serum (100 IU per frog, Calbiochem) approximately 1 week before egg collection. To induce egg laying, primed frogs were injected with human chorionic gonadotropin (400 IU, Calbiochem) and incubated in individual plastic buckets of salt water (13 g NaCl in 2.5 L dH_2O). Eggs were dejellied in 2% cysteine, pH 7.7 (KOH), washed with 0.25X MMR buffer 3 times, then washed with egg lysis buffer 3 times (ELB: 250 mM sucrose, 2.5 mM $MgCl_2$, 50 mM KCl, 10 mM Hepes pH 7.7, 1 mM DTT), and bad eggs were removed. Eggs were packed in 15-ml Falcon tubes (cat # 352059) at 1700 x *g*, excess buffer was removed, and inhibitors were added (cycloheximide 50 μg/ml of eggs; cytochalasin B 2.5 μg/ml, and aprotinin/leupeptin 2.5 μg/ml). Eggs were crushed at

10,000 rpms in an HB4 rotor for 10 minutes. The cytosolic layer was recovered with a 21-gauge needle and 5 ml syringe, and spun again to remove residual pigment and mitochondria. To the crude extract, cycloheximide, aprotinin/leupeptin, cytochalasin B, and DTT were added.

To generate high-speed interphase extracts, crude extract was further spun at 55,000 rpms, 90 minutes in a Beckman TL100 ultracentrifuge in 2.5-ml thin-walled tubes. The top layer of lipids was removed, and the supernatant cytosol was flash-frozen in liquid nitrogen (100 μl/aliquot). The yellow membrane layer was diluted 1:5 in ELB (containing aprotinin, leupeptin, cytochalasin B) mixed by stirring, incubated on ice for 15 minutes, and layered over a 0.2 ml cushion of 0.5 M sucrose in ELB. The membrane fraction was spun through the sucrose cushion at 22,000 rpms for 20 minutes at 2°C. Washed membranes were recovered from the pellet, and flash-frozen in liquid nitrogen (20 μl/aliquot). Sperm heads were purified as described previously [12].

Nuclei were assembled by adding Xenopus sperm heads (2000-5000 per μl of cytosol) to 20 μl of cytosol, with 2 μl of membranes per 20 μl of cytosol, and 0.5 μl of ATP regeneration system per 35 μl of cytosol (ATP regeneration system: 5 μl of 0.2 M ATP in H_2O; 0.5 μl of 5 mg/ml creatine kinase in Hepes pH 7.5, 50% glycerol; 10 μl of 1 M phosphocreatine in phosphate buffer pH 7.0). This mixture was incubated at room temperature and analyzed after 60 and 90 minutes incubation, unless indicated otherwise (timepoints in Figure 2 were 1-10 minutes, 10 minutes, 30 minutes, 45 minutes, 60 minutes, and 90 minutes). Similar results were found at both 60 and 90 minutes in all cases, unless indicated otherwise. Heat-treated, clarified extracts were prepared by boiling cytosolic extract for 1 hour, followed by centrifugation to remove precipitated

proteins. When used to decondense sperm nuclei, no ATP regeneration system was added, and no membranes were added to the extract.

2.3 DNA replication assays

DNA replication assays were performed in triplicate using a final concentration of 0.1 μCi dATP-[α^{32}P] per μl of egg extract. At the indicated time points, reactions were stopped by addition of proteinase K to a final concentration of 1 mg/ml and incubated at 37°C for 1 hour to digest proteins. DNA was separated from unincorporated nucleotide by agarose electrophoresis (1% in TBE buffer). Incorporation of radiolabeled nucleotide was determined by phosphorimaging. Signals were quantitated using ImageJ, and statistics were calculated using Microsoft Excel.

2.4 Antibody generation and usage

CENP-A peptide antibody generation and purification were performed essentially as described previously [13]. CENP-A peptides were synthesized by Zymed Laboratories and conjugated to keyhole limpet hemocyanin (San Francisco, CA). Antibodies were generated in rabbits at the UCSD animal facility. Rabbit anti-UDG antibody was previously characterized [14] and was used at 1:500 for immunofluorescence, and 1:2000 for western analysis. Western analyses were performed as described previously [15].

2.5 Immunofluorescence

Immunofluorescence was performed as described previously [13], with minor changes. Assembled sperm nuclei were resuspended in PBS-Tx (PBS + 0.1% Triton X-100)

containing 10% glycerol and 0.5% formaldehyde. Sperm nuclei were then spun for 10 minutes at 3000 rpm in a clinical centrifuge (2700 x *g*) through a cushion of 25% glycerol in PBS, onto acid-washed coverslips. All blocking solutions contained 5% donkey serum, to maximize dephosphorylation. Data are presented as montages generated using an ImageMagick script developed by BR Chapados, and Adobe Photoshop.

2.6 Imaging and image analysis

Image collection was performed at the UCSD Cancer Center facility, in the laboratory of Dr. James Feramisco, on a Deltavision Deconvolution microscope. All images shown were collected with a 100x Nikon lens, bin=2, pixel size = 0.1032 μm. Each sperm nucleus was imaged in sections of 0.2 μm, at the same exposure time for all samples. These images were then deconvolved using Softworx (Applied Precision) and CENP-A immunofluorescence signals were quantitated using the ImageJ plugin Analyze Particles (Rasband, W.S., ImageJ, National Institutes of Health, Bethesda, Maryland, USA, http://rsb.info.nih.gov/ij/, 1997-2003), with the same thresholds for all images. These data were then compiled and averaged, and errors were calculated using Microsoft Excel. Final data are presented using Cricket Graph. Error bars for all experiments are standard error for the population of cells (at least 5 per experiment) analyzed in at least 3 independent experiments, unless otherwise indicated. Colocalization was determined using Nearcount, a unix program developed by David Nadeau at the San Diego Supercomputer Center. Colocalization data are presented on a per-nucleus basis, where a minimum threshold signal in each channel was required for the spot to be counted.

2.7 Assay for uracil DNA glycosylase activity

Uracil-removal assays were performed using Xenopus egg extracts as the source of uracil-removing activity. Egg extracts (15 μg protein) were preincubated for 10 min on ice in the presence or absence of the indicated antibodies (3 μg) or the PBS2-encoded UNG-inhibitor Ugi (200 ng). Residual UDG activity was assayed by release of [^{3}H]-uracil from a [^{3}H]-U:A-containing calf thymus DNA substrate, and measured by scintillation counting.

2.8 Other reagents

Purified recombinant geminin was supplied by John Newport (UCSD). Purified Ugi and dUTPase were generous gifts from John Tainer (TSRI). Recombinant Ugi was also obtained commercially (upon request) from New England Biolabs. Mutants of human UNG were generated by B Kavli, NTNU, and previously characterized [16]. Nucleotides, dextran sulfate, and Triton-X-100 were from Sigma and Calbiochem (EMD Biosciences). DNA-damaging agents (MNNG, bleomycin) were generous gifts from C Putnam and R Kolodner, Ludwig Institute, UCSD. Cells were irradiated at the UCSD Radiation Facility in the School of Medicine.

3. Results

3.1 Identification and detection of Xenopus CENP-A

Using BLAST and CLUSTALW sequence analysis programs, we identified several potential *X. laevis* CENP-A (XCENP-A) cDNAs. When these potential CENP-A sequences are aligned with known CENP-A proteins from several species, one is ~69%

identical and ~85% similar to human CENP-A (Figure 1A). Based on this similarity, polyclonal rabbit sera were raised against a peptide encoding the N-terminal sequence of the putative XCENP-A (residues 2-20, Figure 1B). A similar peptide has been used previously to generate antisera against human CENP-A [13]. Western blots probing Xenopus egg extract shows that the affinity-purified antibody recognizes a single band, corresponding to the calculated molecular mass of XCENP-A (Figure 1C). Moreover, immunofluorescence staining performed with this antibody detects punctate foci in Xenopus XL177 tissue culture cells (Figure 1D). Similar discrete foci were observed when the antibody was used to stain nuclei that had formed around sperm DNA incubated in Xenopus egg extracts (Figure 1E). CENP-A was not detected on western blots of Xenopus sperm proteins. We suspect that this is because, despite repeated attempts and a variety of methods of decondensation, we were unable to separate CENP-A protein from Xenopus sperm DNA by biochemical or mechanical approaches (data not shown).

3.2 Quantitation of CENP-A foci on Xenopus sperm nuclei

Using 3-dimensional deconvolution microscopy and carefully controlled image collection and analysis, we developed a novel method for quantitating the number of CENP-A foci present in nuclei assembled in egg extract. To do this, sperm nuclei were incubated in egg extract, centrifuged onto coverslips, and processed for detection of CENP-A. Since these nuclei are relatively flat, stacks of 10 images were collected with 0.2 μm separation in the Z-direction, to ensure acquisition of all focal planes before deconvolution. Images were submitted to a set threshold, and spot number was analyzed based on criteria for minimum spot size and intensity (Experimental Procedures). For all

experiments, a minimum of 5 nuclei were quantitated, and each experiment was repeated at least 3 times, unless stated otherwise.

To determine whether CENP-A is present on Xenopus sperm chromatin, the highly condensed sperm were first decondensed by incubation in a dilute dextran sulfate solution, smeared on coverslips and allowed to dry. These coverslips were then processed for detection of CENP-A by indirect immunofluorescence. Under these conditions, the sperm displayed an average of 29 +/- 8 (standard error) CENP-A foci in the absence of added egg extract (Figure 2A and F). In contrast, when decondensation was induced by incubation in egg extract for very short periods of time (10 minutes or less) followed by staining for CENP-A, some of the sperm displayed very few CENP-A foci (data not shown). Since these sperm were qualitatively decondensed to the same degree as that seen with dextran sulfate, this was probably not due to problems with epitope accessibility. Furthermore, we observe that when sperm are decondensed in a clarified, heat-treated egg cytosol, only a small number of CENP-A foci are observed on the decondensed DNA (Figure 2B and F). Comparing the dispersion of the blue color in the figures 2 A and B, it appears that in both cases the DNA is equally decondensed. Therefore, it seems unlikely that CENP-A is undetectable on sperm prepared in heat-treated extract due to incomplete decondensation. It is not surprising that clarified, heat-treated egg cytosol is not competent to assemble CENP-A on sperm DNA, since heating serves two purposes: first, to precipitate the vast majority of proteins, which and are then removed by centrifugation, and second, to decompose, at least partially,the naturally-occurring energy source in the extract (ATP). Thus it is quite striking that clarified heat-treated egg cytosol appears to be competent to remove CENP-A from the sperm DNA.

Although these assays are subject to some variability, there was a consistent trend, as the number of CENP-A foci was found to be different at different timepoints after incubation in egg extract. After 10 minutes of incubation in egg extract, the average number of foci observed is 46 +/- 8 (Figure 2G), and increases to an average of 64 +/- 9 foci by 30 minutes of incubation (Figure 2C and G). These foci do not appear to be aggregates of CENP-A, since they remain bound to the chromatin throughout incubation and washing in PBS containing the detergent triton X-100. The number of foci observed at 30 minutes (64) greatly exceeds the number of anticipated based on the number of chromosomes present in the Xenopus genome (18 haploid, 36 diploid). A likely possibility is that the stockpile of histones present in egg extracts is larger than the pool of CENP-A normally found in somatic cells. This stockpile creates a situation similar to that observed in somatic cells overexpressing CENP-A, where CENP-A is observed bound to DNA along chromosome arms [17].

The number of CENP-A foci declines to 53 +/- 13 foci by 45 minutes of incubation (Figure 2G), and further to 26 +/- 6 foci by 60 minutes (Figure 2D and G), finally reaching equilibrium between 60 and 90 minutes, with an average of 39 foci +/- 10 after 90 minutes of incubation (Figure 2E and G), when DNA replication is essentially complete, as confirmed by a DNA replication assay (Figure 2H). Although we did attempt to follow the sperm nuclei out to 120 minutes of incubation, it is commonly agreed that this cell-free extract system tends to degrade, perhaps due to oxidation, or los activity, through ATP depletion, after 2-3 hours at room temperature. Therefore, we limited our quantitation to the time period when the extract activity is most robust and reproducible.

3.3 Detection of CENP-A foci in the presence of f DNA replication inhibitors

The temporal correlation between the decline in number of CENP-A foci and DNA replication suggested that blocking DNA replication might increase the number of CENP-A foci detectable on sperm after incubation in egg extract. Aphidicolin is an inhibitor of DNA polymerase alpha that blocks both the elongation and initiation phases of DNA replication in Xenopus egg extracts [18]. We observed that addition of aphidicolin to extracts caused a three-fold increase in the number of CENP-A foci at 60 or 90 minutes, relative to untreated sperm nuclei (Figure 3A, B and H). Similarly, when the protein geminin, an endogenous inhibitor that blocks initiation of DNA replication (reviewed in [19]) was added to egg extract, the number of CENP-A foci increased approximately four-fold relative to control nuclei at 60 or 90 minutes (Figure 3C and H). DNA replication assays confirmed that there was no detectable replication in the presence of aphidicolin or geminin (data not shown).

Inhibiting DNA replication can lead to generation of single-stranded DNA and stalled replication forks, which can trigger the DNA damage response. The increased binding of CENP-A observed when replication is inhibited with aphidicolin could be induced by DNA damage. However, geminin is supposed to block DNA replication prior to initiation, and we still observed increased CENP-A binding in the presence of geminin. Therefore, we reasoned that we could be observing endogenous DNA damage that is independent of DNA replication.

3.4 Detection of CENP-A foci in the presence of DNA damaging agents

If endogenous DNA damage is sufficient to increase the number of CENP-A foci in the absence of DNA replication, then we reasoned that deliberately inducing DNA damage could also increase the number of CENP-A foci. To test this possibility, we induced DNA damage in sperm nuclei, and then measured the effect this had on the number of CENP-A foci formed. N-methyl-N'-nitro-N-nitrosoguanidine (MNNG) is a nucleotide analog that incorporates into DNA at the replication fork and activates mismatch repair (reviewed in [20]). Addition of MNNG to the extract (0.5 μg/ml, 3.4 μM) increased the number of CENP-A foci observed by approximately two-fold relative to untreated nuclei (Figure 3D and H). With MNNG treatment, the foci appear to be approximately twice as large as foci detected in untreated nuclei. Ultraviolet light (5 seconds, 265 nm) increased the number of CENP-A foci by approximately four-fold (Figure 3E and H). Bleomycin, a small molecule that binds in the minor groove of DNA and primarily induces double-strand breaks (reviewed in [21]), increased the number of CENP-A foci formed by approximately four-fold (Figure 3F and H). Lastly, a low dose of ionizing radiation (3 Gy) increased CENP-A foci approximately two-fold (Figure 3G and H). Higher doses (10 Gy) increased CENP-A even further, but also interfered with sperm decondensation (data not shown). The foci detected after treatment with bleomycin or irradiation are approximately twice as large, on average, as those in untreated nuclei. Taken together, these data indicate that DNA damage is consistently correlated with an increase in both number and size of CENP-A foci.

3.5 Colocalization of CENP-A foci with UNG2 foci during G2

Recombination at Ig loci appears to be initiated by a deoxycytidine deaminase, which is only active in B-lymphocytes [22], and uracil DNA glycosylase (UDG) [23]. The deoxycytidine deaminase creates uracil in the DNA, which is then removed by UDG. UDG is highly conserved and found in all dividing cells in all kingdoms of life (reviewed in [24]). The nuclear isoform of UDG, UNG2, is present at high levels during S phase, and removes misincorporated uracil during DNA replication. Inexplicably, UNG2 expression increases by 2.8-fold during G2 [25], but at this time UNG2 is concentrated into fewer foci than during S phase [26]. These foci are somewhat reminiscent of CENP-A foci. Therefore, it seemed reasonable to ask whether UNG2 might colocalize with CENP-A foci. To determine whether UNG2 and CENP-A colocalize, we carried out indirect immunofluorescence in Xenopus XL177 tissue culture cells and sperm nuclei assembled in egg extracts. During S phase, a large number of UNG2 foci are distributed along chromatin ([26]; data not shown). During G2, the number of UNG2 foci present on DNA decreases significantly ([26]; data not shown). This change in pattern is sufficiently dramatic that it can be used reliably to determine whether a cell is in S or G2. Using XL177 cells, we observed that when UNG2 is distributed throughout chromatin, it does not colocalize with CENP-A (data not shown). In contrast, during G2, when UNG2 is concentrated in fewer foci, UNG2 and CENP-A are colocalized on chromatin in XL177 cells (Figure 4A and B). The same experiment, which yielded similar results, was also performed using sperm nuclei that had been incubated in egg extract for 90 minutes in order to allow replication to reach completion (Figure 4C and D). Quantitation of the observed nuclei revealed that the percent of UNG2 foci that colocalized with CENP-A is higher in sperm (70%) than in tissue culture cells (50%). In both XL177 cells and sperm

nuclei displaying both UNG2 and CENP-A in punctate patterns, the amount of colocalization ranges from a minimum of 37% to nearly complete (94-100%) colocalization (Figure 4E). Attempts to co-immunoprecipitate CENP-A with UNG2 yielded occasional success, however this was not consistently reproducible, as one might expect from a transient interaction. Alternatively, this may indicate a fragile and/or indirect association between CENP-A and UNG2. Nevertheless, colocalization of UNG2 with CENP-A at the time of CENP-A assembly suggests that UNG2 might have a role in the process of assembling CENP-A on chromatin.

3.6 Assaying UDG catalytic activity in the Xenopus egg extract

To test the possibility that UDG catalytic activity is required for CENP-A assembly, we first assayed the Xenopus egg extract. These assays were performed *in vitro*, using DNA substrates that contain ^{3}H-uracil. Xenopus egg extract was used as the source of UDG activity. Radiolabeled substrate DNA was incubated in the Xenopus egg extract, precipitated, and analyzed by scintillation counting. At least 90% of the uracil-removing activity in the Xenopus egg extracts can be attributed to UNG2, since a UNG-neutralizing antibody [14] blocks most removal of uracil from the substrate DNA, while a control antibody does not (Figure 5A). To completely block UDG activity in a very specific manner, we took advantage of the stoichiometrically binding, UDG-specific bacterial inhibitor protein Ugi (reviewed in [24]). Ugi inhibits all UNG2 homologs, but does not inhibit the other uracil glycosylases TDG, MBD4, cyclin-like UDG and Xenopus SMUG1 [27-29], nor does it inhibit dUTPase or DNA polymerases [30]. Incubation of Xenopus egg extract with purified recombinant Ugi completely blocks

removal of uracil (Figure 5A). Therefore, like chicken DT40 cells, the Xenopus egg extracts used here do not appear to contain a backup UDG activity [31].

3.7 Quantitation of CENP-A foci in the presence of purified enzymes

To begin to differentiate between a requirement for UNG2 binding to DNA as opposed to a requirement for its catalytic activity, a series of purified recombinant mutants of UNG were added to the CENP-A assembly reaction in egg extract (7.5ng/μl final concentration). Addition of wild-type, full-length UNG2, or UNG lacking the unique N-terminus (delta84; [14]) had no effect in extracts containing endogenous full-length UNG2. Similarly, addition of a catalytically dead UNG2 mutant (L242R/D145N; [28]) had no effect in extracts containing endogenous UNG2. However, two mutants that increase the promiscuity of UNG, allowing it to remove cytosine and uracil (Y147A), or thymine and uracil (N204D), both increased the number of CENP-A foci. Finally, addition of the backup uracil DNA glycosylase, hSMUG1, had no effect on the number of CENP-A foci (Figure 5B). These data indicate that promiscuous UNG2 catalytic activity is sufficient to increase the number of CENP-A foci in sperm nuclei.

3.8 Origin of uracil in sperm DNA

Uracil can be incorporated into DNA by promiscuous polymerases, or alternatively it can be generated in the DNA by deamination of deoxycytidine. To differentiate between these two possibilities, we first added purified recombinant human dUTPase to egg extracts (7.5 ng/μl final concentration, a generous gift from JA Tainer). Addition of dUTPase had no effect on CENP-A assembly (Figure 6A, B and J). To test

whether a deoxycytidine deaminase activity is required for CENP-A assembly, we added the specific deoxycytidine deaminase inhibitor, zebularine, to the egg extracts. Quantitation demonstrates that CENP-A foci were not detected in sperm nuclei when zebularine was present in the egg extract at a concentration of 80 μM (Figure 6C and J). Similar results were obtained using another inhibitor of deoxycytidine deaminase, tetrahyrouridine (data not shown). Since zebularine has also been reported to have an effect on DNA methylation, we also tested 5-aza-cytidine, and found that this also had no effect on CENP-A assembly (data not shown). These data suggest that the UDG substrate uracil may be generated in the DNA by a deoxycytidine deaminase, similar to recombination at Ig loci. Consistent with this, addition of dUTP to the egg extract (200–400 μM) was not sufficient to overcome the effect of zebularine (Figure 6D and J). These data support a requirement for deoxycytidine deaminase activity in CENP-A assembly.

To further investigate whether UNG2 enzymatic activity is a requirement for CENP-A assembly into chromatin, Xenopus sperm nuclei were assembled in the presence of the UDG-specific protein inhibitor Ugi (reviewed in [24]). Purified recombinant Ugi from two different sources (New England Biolabs and a generous gift from JA Tainer) was sufficient to induce a loss of detectable CENP-A on sperm nuclear DNA (Figure 6E and J). To verify the specificity of Ugi, we added the much smaller UDG inhibitors uridine triphosphate and uracil. Addition of UTP to the egg extract (250 μM) causes a loss of CENP-A foci (Figure 6F and J), as does uracil at the same concentration (Figure 6G and J), supporting the importance of UDG catalysis. UDG from *E. coli* has a much higher affinity for DNA (two orders of magnitude lower Km than the human enzyme).

Addition of purified recombinant *E. coli* UDG to the extracts greatly increases the number of CENP-A foci (Figure 6H and J). Preincubation of *E. coli* UDG with uracil prevents this increase in CENP-A foci (Figure 6I and J), consistent with a requirement for the catalytic activity of this enzyme.

DNA replication assays revealed that although *E. coli* UDG and uracil inhibited DNA replication, UGI did not completely block DNA replication, and zebularine did not inhibit DNA replication at all (Figure 6K). Thus, although inhibiting UNG2 inhibits DNA replication as well as CENP-A binding to sperm chromatin, zebularine blocks CENP-A binding to sperm chromatin and has no effect on DNA replication.

4. Discussion

CENP-A dynamics on sperm chromatin in Xenopus egg extracts

A characterization of the Xenopus CENP-A protein was very recently published by Edwards and Murray [32]. The amino acid sequence of Xenopus CENP-A described here, is divergent from the sequence reported by Edwards and Murray at the carboxy terminal end. The reason for this divergence is not clear. It should be noted, however that the sequence we report here matches both the human and mouse carboxy termini for an additional 6 residues beyond those reported by Edwards and Murray. Moreover, this difference is likely not relevant to the immunofluorescence detection method used here, since the peptide used for immunization (Figure 1) corresponds to the N-terminus of Xenopus CENP-A.

We chose to use cell-free Xenopus egg extract in order to circumvent the rapid cell death that can result from major perturbations of the DNA replication and repair systems. This is a double-edged sword: the major limitation is that the extracts used here do not execute mitosis or undergo apoptosis. Therefore, the experiments presented here do not demonstrate what the phenotypic consequences might be, if similar experiments were performed with living cells.

The successful use of Xenopus sperm chromatin as a substrate for CENP-A assembly was contingent upon the loss of most, if not all, paternal CENP-A immediately after entry into egg cytoplasm. This phenomenon is currently very difficult to examine in depth, since at present we have no methods that can distinguish the paternal CENP-A protein from the maternal CENP-A protein. However, the observation that incubating sperm in clarified, heat-treated egg cytosol causes an apparent loss of CENP-A from the sperm is consistent with an exchange between paternal CENP-A and the stockpile of egg CENP-A. This could be similar to the exchange of protamines, H2A and H2B that occurs during fertilization in amphibians, as well as in mammals (reviewed in [33]).

The data presented here suggest that CENP-A assembly requires active UNG2. Sperm nuclei treated with UNG inhibitors, such as Ugi, uracil or UTP exhibit a reduced number of CENP-A foci (Figure 5A and 6J). A requirement for active UNG2 predicts that CENP-A assembly is initiated by the product of UNG2 catalysis: an abasic site. It follows that decreasing the number of abasic sites should decrease CENP-A assembly, while increasing the number of basic sites should increase CENP-A assembly. To test this idea, we inhibited deoxycytidine deaminase with the suicide inhibitor, zebularine. This treatment reduces the potential number of abasic sites by decreasing the amount UNG

substrates formed by deamination. Consistent with the proposed mechanism, inhibiting deoxycytidine deaminase blocks formation of CENP-A foci (Figure 6C and J). In contrast, the promiscuous mutant of UNG that can remove cytosine and thymine in addition to uracil induces an increase in the number of CENP-A spots (Fig 5 B) since it generates more products of UNG catalysis (i.e. more abasic sites).

We observed that inhibiting DNA replication is one way to induce a high level of CENP-A assembly on sperm chromatin. There are two possible interpretations of why this might happen. First, we might be inhibiting the second phase of CENP-A dynamics, i.e. the decrease in number of CENP-A foci from 30 to 90 minutes, which parallels the progression of DNA replication (Figure 2). It seems likely that the 'extra' CENP-A detected at 30 minutes of incubation may be degraded[34] and/or replaced with histone H3 during DNA replication. If this is the case, then inhibiting DNA replication would also prevent the replacement step and arrest the process in a stage between initial assembly and subsequent 'cleanup.' Alternatively, inhibiting DNA replication may be inducing more DNA damage, which may recruit more CENP-A to assemble, e.g. at stalled replication forks, Inhibiting DNA replication is not the only way to induce a high level of CENP-A assembly, since other methods of inducing DNA damage also increase the number, and in some cases, size, of CENP-A foci. The increase in focus size is observed with MNNG, bleomycin, and ionizing radiation (proportional to the dose) but not with UNG2 treatment, or with inhibition of DNA replication. The common feature for the three factors that increase the size of CENP-A foci is that they can induce more extensive damage to DNA. The focus size probably correlates with the number of CENP-A molecules bound at that site, which could be consistent with more extensive damage.

Unfortunately, our current assay is limited in that it is not a reliable way to quantitate the number of CENP-A molecules per focus, since it relies on antibody detection. Although some methods of blocking CENP-A assembly also inhibit DNA replication, these processes are clearly not interdependent, since zebularine completely blocks the formation of CENP-A foci on sperm chromatin, but has no effect on DNA replication. Since the involvement of UNG2 supports a requirement for abasic site generation and repair by DNA polymerase beta, we favor the interpretation that CENP-A assembly is independent of DNA replication, but the 'cleanup' phase may be facilitated by DNA replication.

The data presented here support a model for CENP-A assembly that includes dynamic changes in the number of loci upon which CENP-A can be detected. Evidence prior to this had suggested that such a mechanism might exist in somatic cells. Overexpression of epitope-tagged human CENP-A in HeLa cells induces assembly of CENP-A into chromosome arms [17]. Our data demonstrate that promiscuous assembly of CENP-A can be induced on Xenopus sperm chromatin with a variety of DNA damaging methods. These observations may be significant in two ways. First, it is possible that endogenous DNA damage and repair, such as that observed here with UNG2, may be involved in CENP-A assembly *in vivo*. Second, it is possible that CENP-A actually serves a function in DNA repair, perhaps one similar to that played by phosphorylated histone H2AX (reviewed in [35]).

Acknowledgment

Thanks to Chapados BR; Maley F; Goulian M; Kavli, B; Putnam C; Daniels D; Arvai A; Tainer JA; Kolodner R; McMullen S; Monier K; Keck, J; Rosenfeld, R; Harel A; Forbes, D; Harvey, K; Krokan, H; Otterlei, M and Wang JY.

This work was funded in part by NIH NRSA grant # F32 GM069297-01 to SGZ. This work was also supported in part by NIH R01GM33523. GS acknowledges support from The Research Council of Norway, The Norweigian Cancer Society and The Cancer Research Fund at St. Olavs Hospital.

Figure 1. Identification of Xenopus CENP-A.

A, Alignment of Xenopus CENP-A with several known CENP-A homologs: Human, mouse (mus musculus), S. pombe (fission yeast), S. cerevisiae (budding yeast), and Xenopus Laevis. Color scheme represents groups of amino acids: green = basic (R,K,H); yellow = cysteine (C); purple = hydrophobic (L,I,V,M); red = large hydrophobic (F,W,Y); turquoise = acidic or amidic (Q,E,D,N); gray = short side-chains (S,T,A,G,P). **B**, Sequence of peptide used for immunizations. **C**, Western blot demonstrating specificity of the peptide antibody on Xenopus extract. Molecular weight ladder, first lane. Ponceau stain, second lane (left), and antibody detection, second lane (right). **D**, Immunofluorescence demonstrating that the peptide antibody recognizes punctate foci (red) in Xenopus XL177 tissue culture cell nuclei. **E**, nuclei assembled *in vitro* using Xenopus sperm in egg extract. DNA is shown in blue. Red is shown alone (D'-E'). Scalebar = 10 μm.

Figure 2. XCENP-A foci on sperm nuclear DNA.

A-E', Examples of immunofluorescence with the anti-XCENP-A peptide antibody (red). DNA is shown in blue. A-E, merge, A'-E', red channel alone. Scalebar = 10 μm. **A**, Xenopus sperm decondensed with dextran sulfate have detectable CENP-A, consistent with observations from other species. **B**, Xenopus sperm decondensed with boiled egg extract, the main component of which is nucleoplasmin, have very little detectable CENP-A. **C**, CENP-A detected in sperm nuclei after 30 minutes of incubation in egg extracts. **D**, 60 minutes. **E**, 90 minutes. **F and G**, Quantitation from populations of nuclei (error bars shown are standard error). **H,** DNA replication assay. Y axis, lane intensity from phosphorimaging (arbitrary units). X axis, time in minutes.

Figure 3. The number of CENP-A foci increases with DNA damage

A-G', Examples of immunofluorescence with anti-XCENP-A peptide antibody, (red) under various conditions. DNA is in blue, A-G, merge, A'-G', red channel alone. Scalebar = 10 μm. **A**, Control, untreated sperm nuclei. **B**, Sperm nuclei assembled in the presence of aphidicolin. **C**, Sperm nuclei assembled in the presence of purified recombinant geminin. **D**, Sperm nuclei assembled in the presence of MNNG (0.5 μg/ml, 3.4 μM). **E**, Sperm nuclei assembled after treatment with ultra-violet light (time, wavelength). **F**, Sperm nuclei assembled in the presence of bleomycin (0.5 μg/ml). **G**, Sperm nuclei assembled after 3 Gy ionizing radiation. **H**, Quantitation from populations of nuclei.

Figure 4. Uracil DNA Glycosylase (UNG2) transiently colocalizes with CENP-A in somatic and sperm nuclei

A-D', Examples of immunofluorescence with DNA in blue, XCENP-A in red, UNG2 in green. Scalebar = 10 μm. **A-B'**, XL177 Xenopus tissue culture cells. **C-D'**, Xenopus sperm nuclei assembled in egg extracts for 90 minutes. A-D, merge. A'-D', Nearcount masks showing red and green channels equalized for intensity. **E**, Table showing range of overlap between the channels when data is analyzed with Nearcount.

Figure 5. Uracil DNA glycosylase specific activity in Xenopus egg extracts

A, UDG activity assay. DNA substrates containing ^{3}H-labeled uracil were incubated with egg extract (control). The addition of nonspecific IgG has little effect on uracil-removing activity (IgG). Addition of a UNG2-specific neutralizing antibody reduces uracil-removing activity by 90% (Anti-UNG2 IgG). Addition of a specific protein inhibitor of UDG blocks all uracil-removing activity in the extract (Ugi). **B**, Effect on CENP-A assembly of adding purified recombinant UNG2 or UNG mutants to sperm nuclei. Each enzyme was added to a final concentration of 7.5 ng/μl, and CENP-A foci were detected by immunofluorescence and quantitated. No enzyme added (control). Wild-type human full-length UNG2 (WThUNG2) has no effect on the number of CENP-A foci. The catalytic UNG domain lacking the N-terminal regulatory domain (Delta84) has no effect on the number of CENP-A foci. L242R/D145N, the catalytically dead mutant of Delta84, has no effect on the number of CENP-A foci. hSMUG1, a "backup" UDG enzyme, has no effect on the number of CENP-A foci. Y147A, a promiscuous mutant of Delta84 that removes thymidine in addition to uracil, increases CENP-A assembly. N204D, a promiscuous mutant of Delta84 that removes cytosine in addition to uracil, increases CENP-A assembly.

Figure 6. Deoxycytidine deaminase and Uracil DNA glycosylase catalytic activities are required for CENP-A stabilization

A-I', examples of immunofluorescence to detect CENP-A in Xenopus sperm nuclei assembled under various conditions. DNA in blue, CENP-A in red. A-I, merge. A'-I', red channel alone. **A**, Control (untreated). **B**, Purified recombinant dUTPase (7.5 ng/μl final concentration) has no effect on CENP-A assembly. **C**, The deoxycytidine deaminase inhibitor zebularine (80 μM) blocks CENP-A assembly. **D**, Addition of dUTP is not sufficient to overcome the effect of zebularine. **E**, Addition of purified recombinant protein inhibitor of UDG, Ugi, blocks CENP-A assembly. **F** and **G**, UTP and uracil also block CENP-A assembly. **H**, Addition of purified recombinant E. coli UDG increases CENP-A assembly. **I**, Recombinant E. coli UDG pre-incubated with uracil has no effect on CENP-A assembly. **J**, Quantitation from populations of nuclei. **K,** DNA replication assay. Y axis, lane intensity from phosphorimaging (arbitrary units). X axis, time in minutes.

References

[1] E.V. Howman, K.J. Fowler, A.J. Newson, S. Redward, A.C. MacDonald, P. Kalitsis and K.H. Choo Early disruption of centromeric chromatin organization in centromere protein A (Cenpa) null mice, Proc Natl Acad Sci U S A 97 (2000) 1148-1153.

[2] S. Stoler, K.C. Keith, K.E. Curnick and M. Fitzgerald-Hayes A mutation in CSE4, an essential gene encoding a novel chromatin-associated protein in yeast, causes chromosome nondisjunction and cell cycle arrest at mitosis, Genes Dev 9 (1995) 573-586.

[3] V. Regnier, J. Novelli, T. Fukagawa, P. Vagnarelli and W. Brown Characterization of chicken CENP-A and comparative sequence analysis of vertebrate centromere-specific histone H3-like proteins, Gene 316 (2003) 39-46.

[4] P.B. Talbert, T.D. Bryson and S. Henikoff Adaptive evolution of centromere proteins in plants and animals, J Biol 3 (2004) 18.

[5] T. Krude Chromatin assembly during DNA replication in somatic cells, Eur J Biochem 263 (1999) 1-5.

[6] A. Verreault Histone deposition at the replication fork: a matter of urgency, Mol Cell 11 (2003) 283-284.

[7] R.D. Shelby, K. Monier and K.F. Sullivan Chromatin assembly at kinetochores is uncoupled from DNA replication, J Cell Biol 151 (2000) 1113-1118.

[8] R.A. Laskey Chromosome replication in early development of Xenopus laevis, J Embryol Exp Morphol 89 Suppl (1985) 285-296.

[9] J. Newport Nuclear reconstitution in vitro: stages of assembly around protein-free DNA, Cell 48 (1987) 205-217.

[10] D.K. Palmer, K. O'Day and R.L. Margolis The centromere specific histone CENP-A is selectively retained in discrete foci in mammalian sperm nuclei, Chromosoma 100 (1990) 32-36.

[11] K. Katoh, K. Misawa, K. Kuma and T. Miyata MAFFT: a novel method for rapid multiple sequence alignment based on fast Fourier transform, Nucleic Acids Res 30 (2002) 3059-3066.

[12] C. Smythe and J.W. Newport Systems for the study of nuclear assembly, DNA replication, and nuclear breakdown in Xenopus laevis egg extracts, Methods Cell Biol 35 (1991) 449-468.

[13] S.G. Zeitlin, C.M. Barber, C.D. Allis, K.F. Sullivan and K. Sullivan Differential regulation of CENP-A and histone H3 phosphorylation in G2/M, J Cell Sci 114 (2001) 653-661.

[14] G. Slupphaug, I. Eftedal, B. Kavli, S. Bharati, N.M. Helle, T. Haug, D.W. Levine and H.E. Krokan Properties of a recombinant human uracil-DNA glycosylase from the UNG gene and evidence that UNG encodes the major uracil-DNA glycosylase, Biochemistry 34 (1995) 128-138.

[15] S.G. Zeitlin, R.D. Shelby and K.F. Sullivan CENP-A is phosphorylated by Aurora B kinase and plays an unexpected role in completion of cytokinesis, J Cell Biol 155 (2001) 1147-1157.
[16] B. Kavli, G. Slupphaug, C.D. Mol, A.S. Arvai, S.B. Peterson, J.A. Tainer and H.E. Krokan Excision of cytosine and thymine from DNA by mutants of human uracil-DNA glycosylase, Embo J 15 (1996) 3442-3447.
[17] A.A. Van Hooser, Ouspenski, II, H.C. Gregson, D.A. Starr, T.J. Yen, M.L. Goldberg, K. Yokomori, W.C. Earnshaw, K.F. Sullivan and B.R. Brinkley Specification of kinetochore-forming chromatin by the histone H3 variant CENP-A, J Cell Sci 114 (2001) 3529-3542.
[18] K. Marheineke and O. Hyrien Aphidicolin triggers a block to replication origin firing in Xenopus egg extracts, J Biol Chem 276 (2001) 17092-17100.
[19] M. Madine and R. Laskey Geminin bans replication licence, Nat Cell Biol 3 (2001) E49-50.
[20] M. Bignami, M. O'Driscoll, G. Aquilina and P. Karran Unmasking a killer: DNA O(6)-methylguanine and the cytotoxicity of methylating agents, Mutat Res 462 (2000) 71-82.
[21] S.M. Hecht Bleomycin: new perspectives on the mechanism of action, J Nat Prod 63 (2000) 158-168.
[22] M. Muramatsu, V.S. Sankaranand, S. Anant, M. Sugai, K. Kinoshita, N.O. Davidson and T. Honjo Specific expression of activation-induced cytidine deaminase (AID), a novel member of the RNA-editing deaminase family in germinal center B cells, J Biol Chem 274 (1999) 18470-18476.
[23] J. Di Noia and M.S. Neuberger Altering the pathway of immunoglobulin hypermutation by inhibiting uracil-DNA glycosylase, Nature 419 (2002) 43-48.
[24] C.D. Putnam, M.J. Shroyer, A.J. Lundquist, C.D. Mol, A.S. Arvai, D.W. Mosbaugh and J.A. Tainer Protein mimicry of DNA from crystal structures of the uracil-DNA glycosylase inhibitor protein and its complex with Escherichia coli uracil-DNA glycosylase, J Mol Biol 287 (1999) 331-346.
[25] T.A. Nagelhus, G. Slupphaug, T. Lindmo and H.E. Krokan Cell cycle regulation and subcellular localization of the major human uracil-DNA glycosylase, Exp Cell Res 220 (1995) 292-297.
[26] M. Otterlei, E. Warbrick, T.A. Nagelhus, T. Haug, G. Slupphaug, M. Akbari, P.A. Aas, K. Steinsbekk, O. Bakke and H.E. Krokan Post-replicative base excision repair in replication foci, Embo J 18 (1999) 3834-3844.
[27] H. Nilsen, K.A. Haushalter, P. Robins, D.E. Barnes, G.L. Verdine and T. Lindahl Excision of deaminated cytosine from the vertebrate genome: role of the SMUG1 uracil-DNA glycosylase, Embo J 20 (2001) 4278-4286.
[28] B. Kavli, O. Sundheim, M. Akbari, M. Otterlei, H. Nilsen, F. Skorpen, P.A. Aas, L. Hagen, H.E. Krokan and G. Slupphaug hUNG2 is the major repair enzyme for removal of uracil from U:A matches, U:G mismatches, and U in single-stranded DNA, with hSMUG1 as a broad specificity backup, J Biol Chem 277 (2002) 39926-39936.
[29] K.A. Haushalter, M.W. Todd Stukenberg, M.W. Kirschner and G.L. Verdine Identification of a new uracil-DNA glycosylase family by expression cloning using synthetic inhibitors, Curr Biol 9 (1999) 174-185.

[30] Z. Wang and D.W. Mosbaugh Uracil-DNA glycosylase inhibitor gene of bacteriophage PBS2 encodes a binding protein specific for uracil-DNA glycosylase, J Biol Chem 264 (1989) 1163-1171.
[31] J.M. Di Noia and M.S. Neuberger Immunoglobulin gene conversion in chicken DT40 cells largely proceeds through an abasic site intermediate generated by excision of the uracil produced by AID-mediated deoxycytidine deamination, Eur J Immunol 34 (2004) 504-508.
[32] N.S. Edwards and A.W. Murray Identification of Xenopus CENP-A and an Associated Centromeric DNA Repeat, Mol Biol Cell (2005).
[33] D.W. McLay and H.J. Clarke Remodelling the paternal chromatin at fertilization in mammals, Reproduction 125 (2003) 625-633.
[34] K.A. Collins, S. Furuyama and S. Biggins Proteolysis contributes to the exclusive centromere localization of the yeast Cse4/CENP-A histone H3 variant, Curr Biol 14 (2004) 1968-1972.
[35] C. Redon, D. Pilch, E. Rogakou, O. Sedelnikova, K. Newrock and W. Bonner Histone H2A variants H2AX and H2AZ, Curr Opin Genet Dev 12 (2002) 162-169.

A

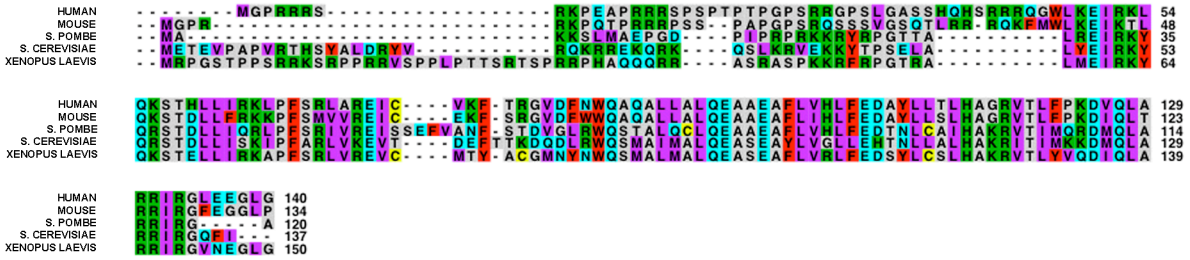

B RPGSTPPSRRKSRPPRRVS

C

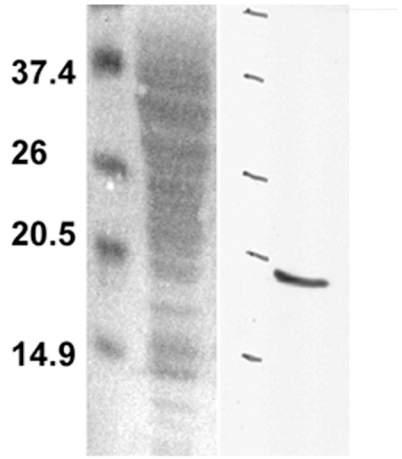

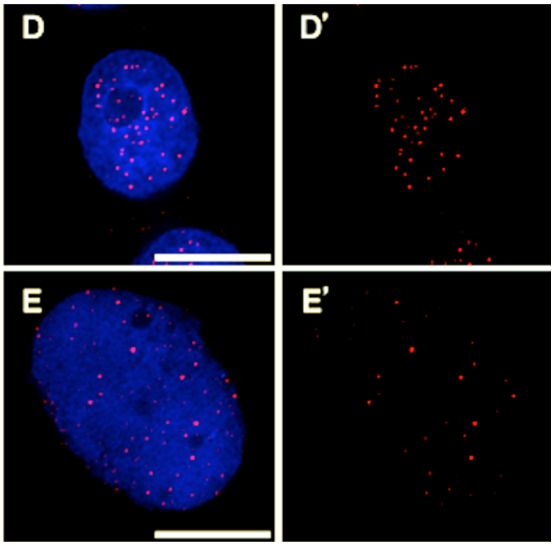

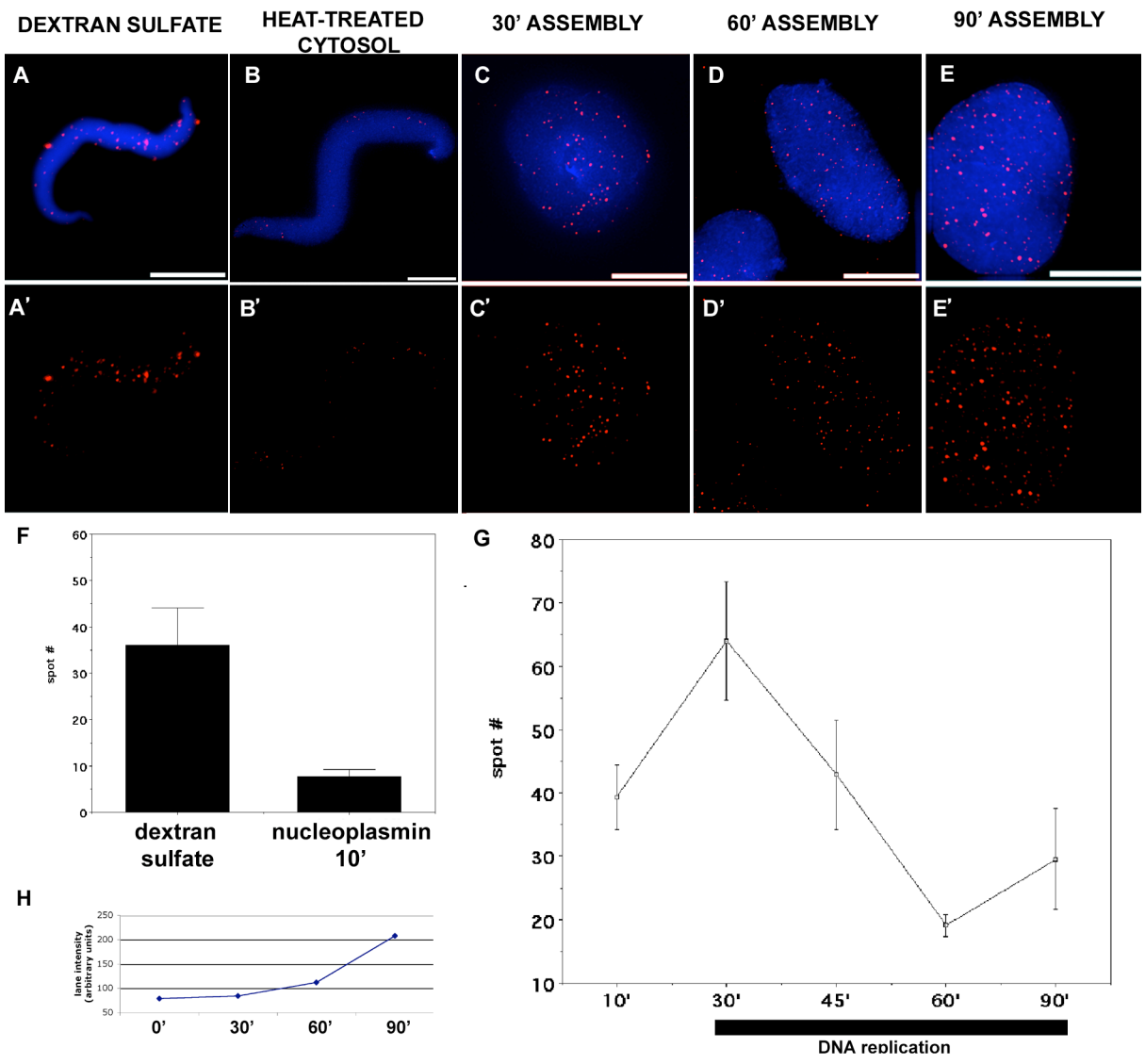
DEXTRAN SULFATE
HEAT-TREATED CYTOSOL
30' ASSEMBLY
60' ASSEMBLY
90' ASSEMBLY
A
B
C
D
E
A'
B'
C'
D'
E'
F
spot #
dextran sulfate
nucleoplasmin 10'
G
spot #
10'
30'
45'
60'
90'
DNA replication
H
lane intensity (arbitrary units)
0'
30'
60'
90'

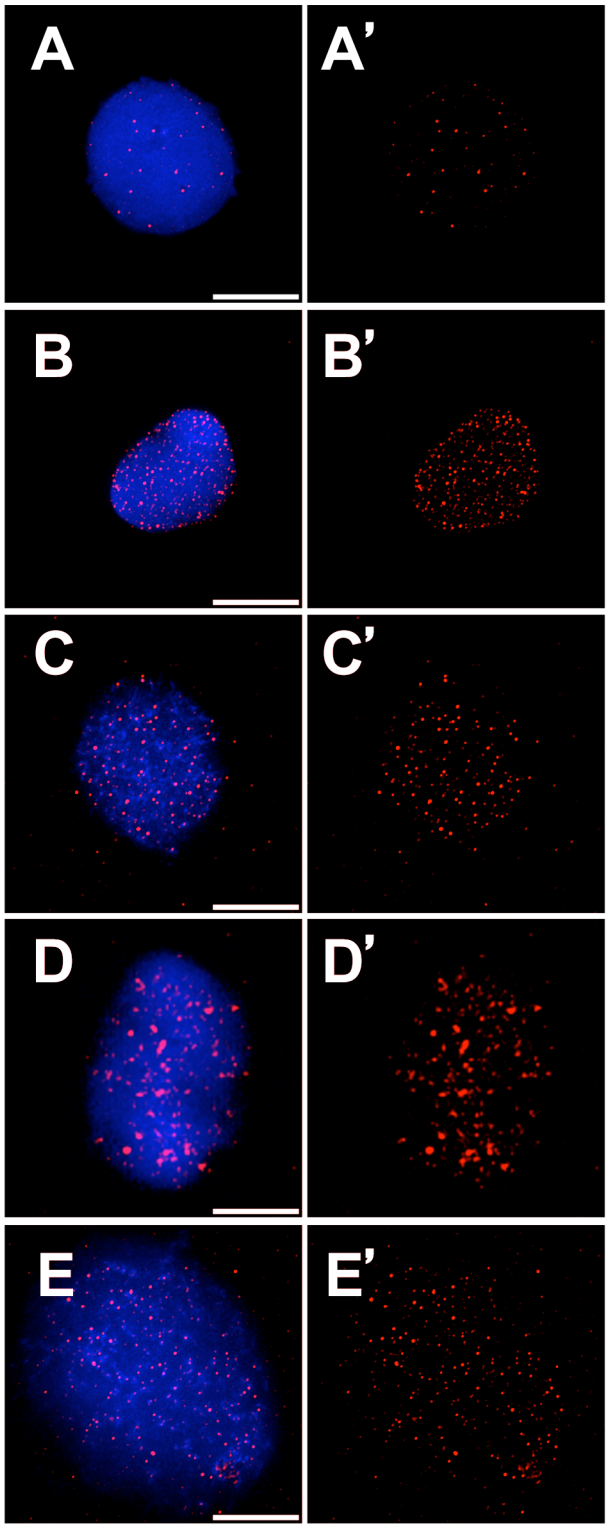
A
A'
B
B'
C
C'
D
D'
E
E'

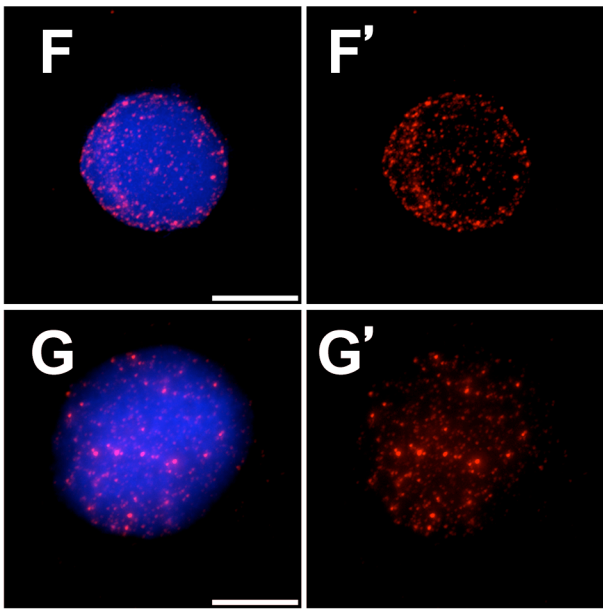
F
F'
G
G'

H

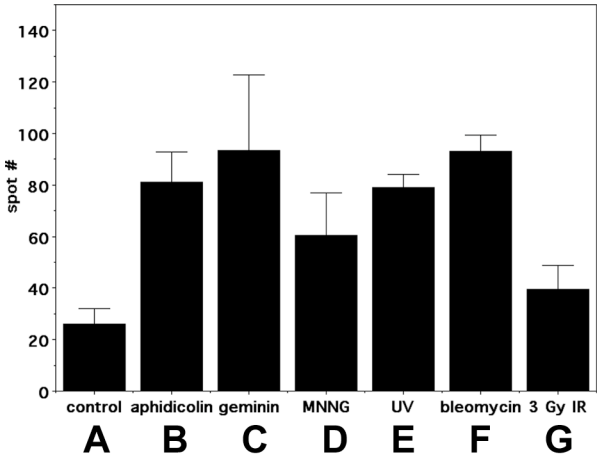
spot #
140
120
100
80
60
40
20
0
control
aphidicolin
geminin
MNNG
UV
bleomycin
3 Gy IR
A
B
C
D
E
F
G

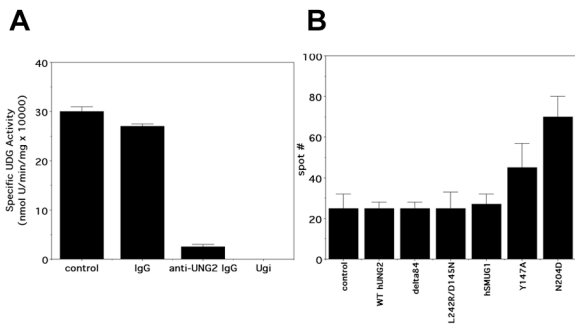
A
B
Specific UDG Activity
(nmol U/min/mg x 10000)
40
30
20
10
0
control
IgG
anti-UNG2 IgG
Ugi
spot #
100
80
60
40
20
0
control
WT hUNG2
delta84
L242R/D145N
hSMUG1
Y147A
N204D

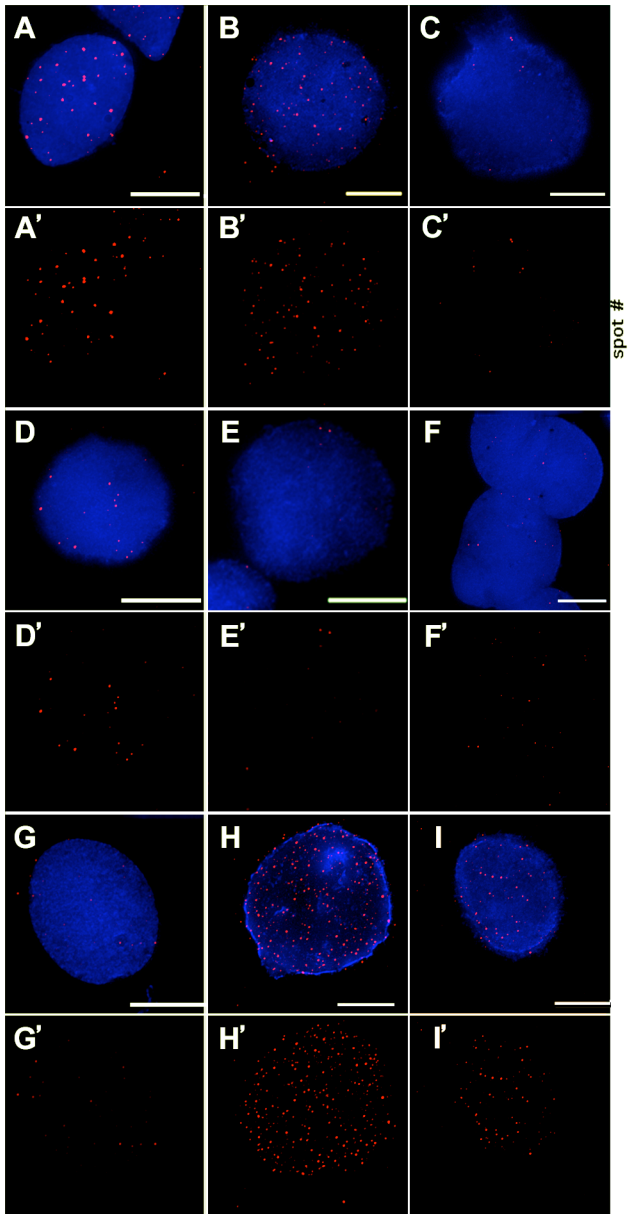
A
B
C
A'
B'
C'
D
E
F
D'
E'
F'
G
H
I
G'
H'
I'

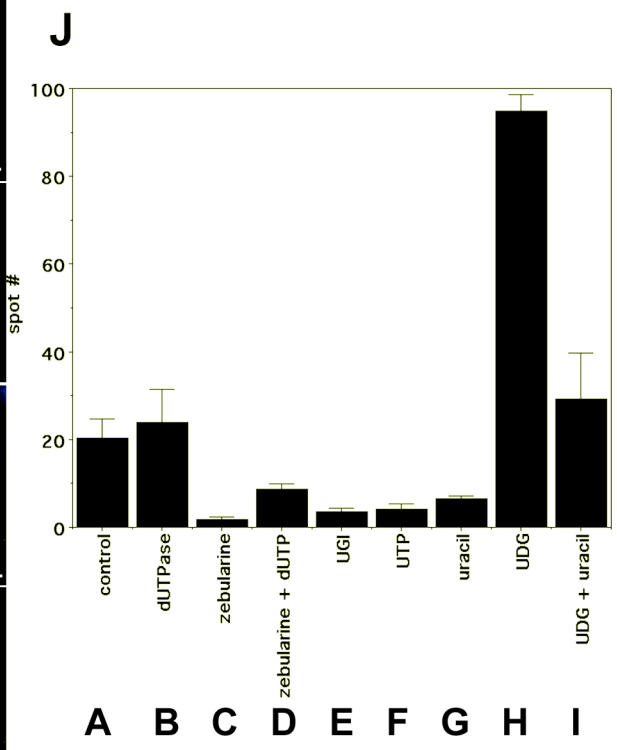
J
spot #
100
80
60
40
20
0
control
dUTPase
zebularine
zebularine + dUTP
UGI
UTP
uracil
UDG
UDG + uracil
A B C D E F G H I

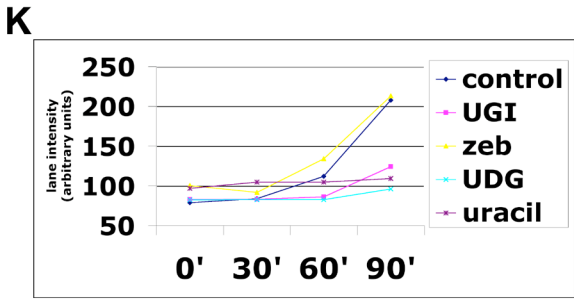
K
lane intensity (arbitrary units)
250
200
150
100
50
0' 30' 60' 90'
control
UGI
zeb
UDG
uracil